

Low-Temperature Methane Activation under Nonoxidative Conditions over Supported Ruthenium–Cobalt Bimetallic Catalysts

L. Guczi, K. V. Sarma, and L. Borkó

Department of Surface Chemistry and Catalysis, Institute of Isotopes of the Hungarian Academy of Sciences, P.O. Box 77, H-1525 Budapest, Hungary

Received July 3, 1996; revised November 4, 1996; accepted January 3, 1997

Dissociative chemisorption of methane over ruthenium, cobalt, and ruthenium–cobalt bimetallic catalysts supported by alumina, silica, and NaY was investigated under a wide range of temperatures. The extent of hydrogen loss from methane was monitored by deuterium uptake of the surface carbonaceous species (CH_x) formed from methane and/or by the amount of hydrogen evolved during the course of methane chemisorption. The presence of a high average number of deuteriums in the desorbing methane suggested a wide spread dissociation of methane. The initial distribution of the deuterated products generally decreased in the sequence $\text{CD}_4 > \text{CHD}_3 > \text{CH}_2\text{D}_2$. The amount of chemisorbed methane and the evolution of hydrogen during methane chemisorption increase with temperature and follow the sequence of reducibility of the supported metals and the particle size which, in turn, depends on the support and the alloy formed. CH species prevailed on alumina- and silica-supported catalysts, while on NaY-supported metals, CH_2 species are dominant when small metal particles are stabilized inside the supercage.

© 1997 Academic Press

1. INTRODUCTION

C–H bond activation in methane, the first step in the “two-step reaction” applied for the low-temperature nonoxidative methane coupling, is of current interest (1–4). The thermodynamically dictated large gap between the temperatures applied for chemisorption of methane and that used in subsequent hydrogenation is one of the drawbacks of this process. Furthermore, when C–H bond cleavage occurs at too high temperature, hydrogen-free carbon atoms are transformed easily into nonreactive carbon species which become spectator molecules on the surface. It is, therefore, of primary interest to decrease the temperature of methane dissociative chemisorption to avoid the undesirable side reactions in the methane low-temperature coupling (5–7). In order to facilitate C–H bond rupture during methane chemisorption, proper catalysts should be selected.

The surface CH_x species formed from methane, contains some amount of hydrogen. When x is equal to zero, or large (e.g., $x=3$) the respective surface CH_x species

are transformed into a spectator species, or is not reactive enough to build up higher hydrocarbons. The x values could be estimated by the deuterium uptake by CH_x and can be measured by analyzing the deuterium content in the $\text{CH}_x\text{D}_{(4-x)}$ molecule. Hence, on the basis of the average deuterium number (M_D) in the forming deuterated methane the amount of hydrogen retained by the surface carbon atoms can be estimated. Similar experiments have been carried out by Tanaka *et al.* over cobalt catalysts (8).

Cobalt and ruthenium manifested themselves in the nonoxidative coupling of methane to have higher activity than other platinum group metals (1, 2, 9). In addition to the nature of metals and the role of support (10–13), the extent of reduction of the metal ions is one of the major factors which affects the activity of a catalyst in C–H bond cleavage. Conversely, the extent of reduction depends on the particle size (5) as was found to be valid for supported cobalt samples (6). Reduction of the cobalt ions inserted in a zeolite matrix is difficult (14, 15), but it is relatively easy when deposited on alumina support (16). However, the reducibility of the cobalt ions in zeolite can be significantly facilitated when platinum is added to the system (17). In addition to the enhanced reducibility, modification of the metallic cobalt by platinum in bimetallic particles is also expected. Methane chemisorption increased significantly on the platinum–cobalt bimetallic particles formed in the Pt–Co/NaY system (5, 6). Similar effect was reported in the rhodium–copper samples (18).

In the present work we wanted to find relationships between the dissociative chemisorption of methane and methane coupling on well-characterized alumina-, silica-, and zeolite-supported ruthenium and cobalt samples reported in the accompanying paper (19). The key issue is the reducibility of the supported cobalt ions into metallic cobalt particles which can be facilitated by the presence of ruthenium. In addition to the effect of ruthenium–cobalt bimetallic particles, of the pretreatment conditions on the C–H bond rupture in methane is also the subject of our studies. The chemisorption process is complemented by measuring the amount of hydrogen evolved and an attempt is made to make correlation with the result of deuterium uptake.

2. EXPERIMENTAL

2.1. Catalyst Preparation

Catalysts supported on alumina and silica were prepared by incipient wetness method using aqueous solutions of $\text{Ru}(\text{NH}_3)_6\text{Cl}_3$ and $\text{Co}(\text{NO}_3)_2$. Bimetallic samples were prepared by coprecipitation using the solution of both precursors. The preparation of the Co/NaY , Ru-Co/NaY , and Ru/NaY was carried out by ion-exchange method. Two types of bimetallic catalysts were prepared: in the Ru-Co/NaY [I] sample first $\text{Co}(\text{NO}_3)_2$ and then $\text{Ru}(\text{NH}_3)_6\text{Cl}_3$ were introduced and in the Ru-Co/NaY [III] sample the sequence of exchange was reversed. All samples were first dried in air at room temperature and then at 100°C for 2 h. The samples were calcined in a stream of oxygen at 300°C for 2 h, while decomposition of the ruthenium complex in NaY was carried out in helium ($40 \text{ cm}^3/\text{min}$). Reduction of the samples was carried out in a stream of H_2 ($40 \text{ cm}^3/\text{min}$) at 450°C . The entire procedure was detailed previously (19). Metal loading was in the range of 2.5 to 5.0 wt% cobalt or ruthenium, determined by XRF technique.

The purity of methane used was 99.999%. Deuterium (with 99.5% purity) and hydrogen gases were further purified by diffusion through heated palladium–silver thimble.

2.2. Experimental Method

Chemisorption of methane was studied in an all glass circulating system connected to a KRATOS MS 20 mass spectrometer via a capillary leak to ensure a viscous flow into the mass spectrometer. The circulating apparatus including the capillary leak were heated to 60°C during chemisorption.

The *in situ* sample preparation, including calcination at 300°C in a stream of oxygen for 1 h (for the NaY -supported ruthenium calcination was replaced by helium treatment) followed by reduction in a stream of hydrogen at $400\text{--}450^\circ\text{C}$ for 10 h (2 h in case of ruthenium samples) was a standard procedure. Following the reduction, the samples were evacuated at 400°C for 2 to 3 h until the pressure dropped below $2 \times 10^{-3} \text{ Pa}$. The temperature was then adjusted to that used for methane chemisorption. Generally 1.3 kPa methane ($102.5 \mu\text{mol}$ in the reaction volume of 187 cm^3) was admitted to the catalyst sample at different temperatures and circulated usually for 3 min. Simultaneously, evolution of hydrogen ($m/e = 2$) during chemisorption was recorded. After finishing chemisorption the system was evacuated.

The amount of methane chemisorbed in the form of CH_x at different temperatures was determined by removing the CH_x surface species by oxidation in a stream of oxygen at 300°C . The CO_2 trapped at liquid nitrogen temperature was allowed to warm up; then the pressure was adjusted to 13 kPa using helium, and the CO_2 was determined by means of a mass spectrometer.

In separate experiments deuterium was used instead of hydrogen to remove the CH_x surface species in the form of $\text{CH}_x\text{D}_{(4-x)}$ by adding 13 kPa deuterium to the catalyst at 100°C . All analyses were performed at 13 kPa total pressure due to the viscous flow into the mass spectrometer. The intensity of the six peaks corresponding to the ions at $m/e = 15$ to 20 were measured at given intervals throughout the course of CH_x removal in deuterium. The peak intensities were corrected for the background in the spectrometer, naturally occurring ^{13}C and natural deuterium abundance in methane. The average number of deuterium atoms in the resulting $\text{CH}_x\text{D}_{(4-x)}$ molecules, M_D , was calculated by $M_D = \sum id_i$, where d_i is the percentage of the methane molecules containing i number of deuterium atoms (20).

Although fragmentation of heavy and light methane is not identical, earlier experiments showed that by using the same pattern of fragmentation for CH_4 and CD_4 , the error does not exceed 10%. The heights of the various peaks, thus corrected, represent the relative proportion of each of the deuterated methane species.

3. RESULTS

3.1. Factors Disturbing the Determination of Deuterium Content in Methane

In order to classify a catalyst in methane chemisorption, it is crucial to determine the hydrogen content in the CH_x surface species formed in the first step chemisorption carried out at various temperatures. This was estimated in the subsequent hydrogenation (second step) carried out at 100°C (if not stated otherwise) when deuterium is applied instead of hydrogen to determine the x value in the deuterated methane, $\text{CH}_x\text{D}_{(4-x)}$ formed. However, this is valid only if no side reaction takes place. There are two important factors which might interfere with this method and could cause a side effect: (i) postexchange of the gaseous $\text{CH}_x\text{D}_{(4-x)}$ with deuterium under the conditions used for deuterium uptake, and (ii) deuterium exchange between protons in the support hydroxyl groups and gaseous deuterium. The former would increase, the latter could decrease in the deuterium content of the $\text{CH}_x\text{D}_{(4-x)}$ because of the dilution of the gas phase deuterium. In order to demonstrate the absence of these effects under the conditions applied, experiments were carried out and the results are presented in Figs. 1 and 2.

First, the exchange between methane and deuterium at various temperatures was carried out over $\text{Co/Al}_2\text{O}_3$. A mixture of $102.5 \mu\text{mol}$ methane and $1025 \mu\text{mol}$ deuterium was introduced, and the exchange was followed at 100°C by monitoring the change in the peak intensities in the methane- d_0 to methane- d_4 products. The temperature was then increased and, as shown in Fig. 1, the percentage of methane- d_0 started decreasing above 200°C with a simultaneous increase in the percentage of methane- d_1

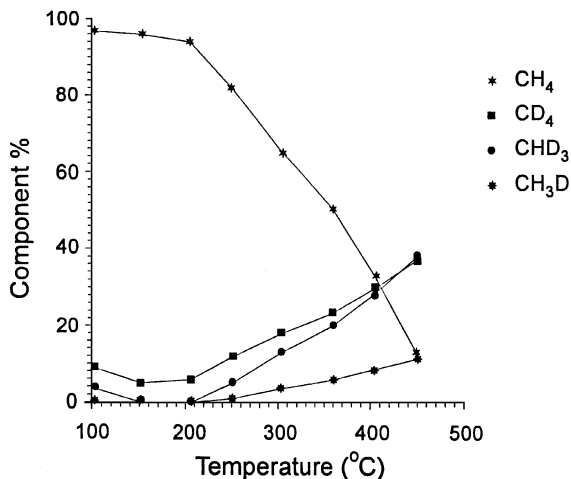


FIG. 1. Methane deuterium exchange over Co/Al₂O₃ sample at various temperatures.

to methane-d₄. These results illustrate that additional hydrogen/deuterium exchange in methane rarely occurs below 200°C.

Dilution of the deuterium gas with hydrogen might result from the OH groups of the support. This effect was investigated over a Pt/SiO₂ sample, because on metallic platinum, deuterium can easily be activated; hence it should be the bottom line for exchange. In Fig. 2 the HD/D₂ ratio is plotted vs temperature. The ratio is low and constant up to about 400°C when it starts increasing. Consequently, the deuterium uptake in CH_x is not affected by dilution of deuterium gas.

3.2. Hydrogen Content in CH_x over Cobalt and Ruthenium Catalysts

First, dissociative chemisorption of methane on Co/Al₂O₃, Co/SiO₂, and Co/NaY samples was studied. Typical

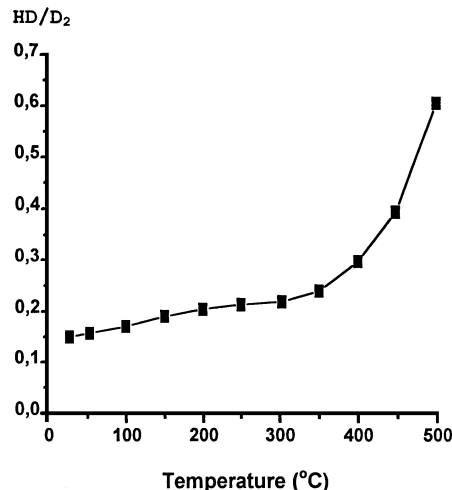


FIG. 2. HD/D₂ ratio vs temperature over a Pt/SiO₂ catalyst.

TABLE 1

Composition of Deuterated Methane Formed over Co/Al₂O₃ at 100°C and M_D Values for Co/Al₂O₃, Co/SiO₂, and Co/NaY Samples

T (°C) ^a	Deuterated methane (%)				M_D		
	d ₁	d ₂	d ₃	d ₄	Al ₂ O ₃	SiO ₂	NaY
250	0	12	29	47	2.9	—	0.8
300	0	8	31	47	2.9	—	1.2
350	0	8	27	57	3.1	3.1	1.4
400	0	10	29	52	3.2	3.2	2

^a Chemisorption temperature of methane.

data measured over Co/Al₂O₃ for the initial percentage distribution of methane-d₁ to methane-d₄ at different temperatures are given in Table 1. The main product is methane-d₄, irrespective of the temperature, indicating the high degree of hydrogen dissociation during methane chemisorption. Similar results were obtained for Co/SiO₂, whereas the dissociation is considerably lower on the Co/NaY sample.

The average deuterium number (M_D) in the desorbing methane molecules appeared to be more characteristic of the hydrogen content in the surface CH_x species. The values on various cobalt catalysts showed that the amount of highly dissociated surface CH_x species slightly increased with temperature (Table 1).

Typical curves representing the total amount of methane chemisorbed and the production of hydrogen at different temperatures are plotted in Figs. 3 and 4, respectively. Hydrogen evolution was observed at temperatures as low as 250°C on Co/Al₂O₃. Methane chemisorption was strongly

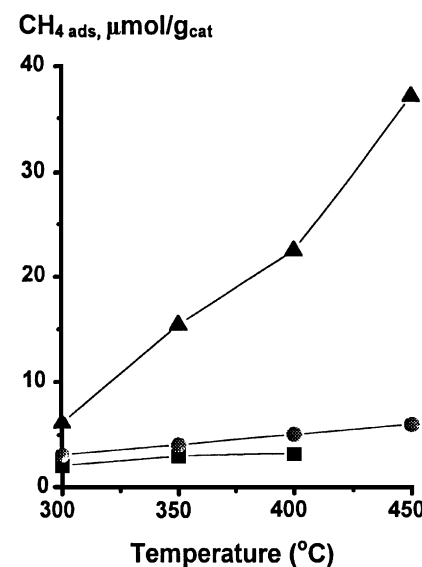


FIG. 3. Methane chemisorption over various catalysts as a function of temperature (■) Co/NaY; (●) Co/SiO₂; (▲) Co/Al₂O₃.

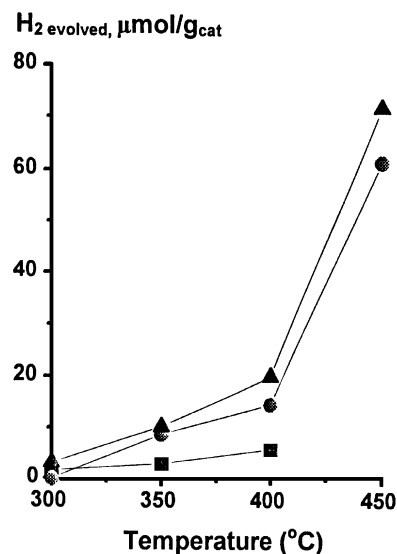


FIG. 4. Hydrogen evolution vs temperature during methane chemisorption over various catalysts. (■) Co/NaY; (●) Co/SiO₂; (▲) Co/Al₂O₃.

influenced by the nature of the support. The most active catalyst for both methane chemisorption and hydrogen evolution was Co/Al₂O₃, followed by Co/SiO₂ and Co/NaY. The amounts of both methane chemisorbed and hydrogen evolved increased with increasing temperature. On the zeolite-supported sample only a small amount of methane was chemisorbed (2 μmol/g_{cat}) at 250°C, and the hydrogen evolved was almost zero which was due to the low degree of reduction of Co²⁺ ions in zeolite (19).

Distribution of the deuterium atoms in the methane formed after deuterium uptake over alumina- and silica-supported ruthenium catalysts is shown in Table 2. On Ru/SiO₂ and Ru/Al₂O₃, the amounts of highly deuterated species indicated by M_D values are slightly lower

than the corresponding amounts measured over the cobalt samples.

In the case of the helium-treated Ru/NaY sample, the deuterium distribution measured at 250°C was CH₂D₂ (13%), CHD₃ (59%), and CD₄ (26%) (5), whereas for the oxygen-treated samples at the same temperature the respective values were 47, 44, and 8%.

3.3. Hydrogen Content in CH_x over Supported Ruthenium-Cobalt Samples

The composition of deuterated methane formed over Ru-Co/SiO₂ and Ru-Co/Al₂O₃ samples after deuterium uptake of CH_x is shown in Table 3. As described in the previous sections, the percentage of methane-d₄ is the highest of the products formed. Low and/or zero percentages of methane-d₁ in both alumina- and silica-supported samples indicated the high extent of hydrogen dissociation from methane. As shown in Table 3, dissociative chemisorption of methane took place on alumina-supported samples to a greater extent than on silica-supported samples. This was also reflected in the average deuterium number (M_D) presented in Table 3. Over alumina- and silica-supported samples the M_D value increased with increasing temperature.

The amount of chemisorbed methane on Ru-Co/SiO₂ was higher than on Ru-Co/Al₂O₃ and increased with temperature (Table 3). Furthermore, the amount of methane chemisorbed on Ru-Co/SiO₂ system was higher than that on Ru/SiO₂. The same is valid for the corresponding alumina-supported catalysts. The amount of the hydrogen evolved in the dissociative chemisorption of methane also increased with temperature (Table 3). The hydrogen evolved more or less corresponds to that calculated from the methane chemisorbed and the value determined from deuterium uptake. Deviation becomes significant only at high temperature on Ru-Co/Al₂O₃ which can be explained by the extra source of hydrogen (e.g., activated hydrogen chemisorption or metal/proton interaction).

3.4. Hydrogen Content in CH_x over Ru-Co/NaY Zeolite Sample

As indicated in the accompanying paper (19), in the Ru-Co/NaY[II] sample treated in helium and reduced in a

TABLE 2
Composition of Deuterated Methane Formed from CH_x
and M_D Values over Ruthenium Samples

T (°C)	Deuterated methane (%)				
	d ₁	d ₂	d ₃	d ₄	M_D
Ru/Al ₂ O ₃					
250	0	14	28	40	2.7
300	0	14	29	43	3
350	0	14	29	45	2.9
400	0	10	27	48	3
450	0	14	29	50	2.9
Ru/SiO ₂					
300	17	20	35	32	2.9
350	6	10	31	41	3
400	0	13	26	46	2.9
450	0	11	29	48	3

TABLE 3
Composition of Deuterated Methane Formed and M_D Values
over SiO₂- and Al₂O₃-Supported Bimetallic Samples

T (°C)	Ru-Co/SiO ₂				Ru-Co/Al ₂ O ₃							
	d ₂	d ₃	d ₄	M_D (μmol/g)	CH ₄ (μmol/g)	H ₂ (μmol/g)	d ₂	d ₃	d ₄	M_D (μmol/g)	CH ₄ (μmol/g)	H ₂ (μmol/g)
300	21	35	21	2.3	15	15	9	23	42	2.5	6	15
350	15	38	30	2.6	23	26	10	30	46	2.9	16	25
400	25	43	17	2.5	30	49	20	38	34	2.9	17	98

TABLE 4

Composition of Deuterated Methane Formed from CH_x over a Ru-Co/NaY[I] Catalyst (He-Treated Sample)

T (°C)	Deuterated methane (%)				M_D	M_D^a
	d_1	d_2	d_3	d_4		
150	5	21	25	17	1.9	NA
200	6	8	29	23	2.0	NA
250	9	25	31	31	2.3	3.07
300	0	3	27	46	2.8	3.05

^a Ru/NaY zeolite treated in helium. M_D 350°C is 3.03 and data for other temperatures are not available.

stream of hydrogen, small metal particles formed which are highly active in C–H bond breaking in methane chemisorption (5–7). The effect of particle size was studied in separate experiments when, after He/H₂ treatment, the sample was calcined in oxygen. The amount of methane chemisorbed was higher on helium-treated samples than on oxygen-treated samples. It was reflected by the difference between the amounts of hydrogen detected in the gas phase during methane chemisorption which changed in a way parallel to methane chemisorption. The amounts of methane chemisorbed on helium- and oxygen-treated Ru-Co/NaY[I] samples were somewhat higher than those measured over the Ru/NaY sample.

The initial product distributions of deuterated methane for helium- and oxygen-treated samples are given in Tables 4 and 5, respectively. Although there is migration of ruthenium to the external surface in the presence of oxygen, the Ru-Co/NaY[II] sample shows a higher activity than the corresponding Co/NaY and Ru/NaY samples.

The initial product distributions of the deuterated methane and the M_D value at 250°C obtained on Ru-Co/NaY[II] are given in Table 6. The chemisorption of methane was carried out on (i) the sample treated in helium followed by reduction in hydrogen, (ii) the sample calcined directly in oxygen followed by reduction, and (iii) the sample treated in helium first then in oxygen fol-

TABLE 6

Composition of Deuterated Methane Formed and M_D Values over Ru-Co/NaY[II] Sample

T (°C) ^a	Deuterated methane (%)				M_D
	d_1	d_2	d_3	d_4	
250/250 (He)	0	21	42	12	2.2
250/250 (O ₂)	0	15	59	26	3.1
250/250 (O ₂) ^b	0	0	51	31	2.8

^a The second temperature is the deuteration temperature.

^b Direct oxidation.

lowed by reduction in hydrogen. In case (i) the amount of methane chemisorbed and the hydrogen evolved were 10 and 7 $\mu\text{mol/g}_{\text{cat}}$, respectively. In case (ii) the amount of methane chemisorbed was very low, but the extent of methane dissociation represented by M_D was 2.2 and 2.8 for helium- and oxygen-treated samples, respectively. In case (iii) there was the least probability of ruthenium migrating to the external surface. In this case the methane chemisorption must increase which is what we found. The amount of hydrogen evolved in this case (He/O₂-treated sample) was 25 $\mu\text{mol/g}_{\text{cat}}$, whereas in the first case it was only 10 $\mu\text{mol/g}_{\text{cat}}$. Therefore, repeated helium–oxygen treatments greatly increased the activity of the catalyst and such a system not only had an increased methane chemisorption, but also an increased C–H bond cleavage, which was reflected in the average deuterium number, M_D , being 2.2 and 3.1 for helium-treated and helium–oxygen-treated samples, respectively.

The amount of methane chemisorbed on oxygen-treated Ru/NaY was about 5 $\mu\text{mol/g}_{\text{cat}}$, whereas on Ru-Co/NaY[II] the amount of methane chemisorbed was less than 1 $\mu\text{mol/g}_{\text{cat}}$. The amount of hydrogen evolved on the Ru/NaY sample, oxygen-treated, amounted to around 6 $\mu\text{mol/g}_{\text{cat}}$, whereas on the bimetallic system it was less than 5 $\mu\text{mol/g}_{\text{cat}}$.

4. DISCUSSION

Although a small increase in the intensity at mass $m/e = 30$ was observed during methane chemisorption, it cannot unambiguously be regarded as coupling products under the methane chemisorption. It could be ascribed to the presence of hydrogen in the circulating methane during chemisorption. Second, as shown in the methane/deuterium and hydrogen/deuterium exchange experiments, no additional change in the deuterium distribution of methane occurs during the deuteration of the CH_x surface species at about 100°C. Therefore, we are confident that the deuterium distribution reflects the hydrogen content of the CH_x species removed in the form of $\text{CH}_x\text{D}_{(4-x)}$.

TABLE 5

Composition of Deuterated Methane Formed over Ru-Co/NaY[I] Catalyst (O₂-Treated Sample)

T (°C)	Deuterated methane (%)				M_D	M_D^a
	d_1	d_2	d_3	d_4		
150	5	27	17	17	1.8	
200	0	26	15	24	1.9	
250	6	44	33	28	2.2	2.4
300	0	13	28	40	2.7	2.6

^a Ru/NaY zeolite treated in oxygen. M_D at 350°C is 2.56; data for other temperatures are not available.

The M_D values show a slow trend toward higher values with increasing temperature. The curves plotted in Figs. 3 and 4, however, indicate a rather drastic increase both in the amount of chemisorbed methane and in the hydrogen evolved. The most likely explanation is that with increasing temperature, a part of the CH_x species dissociate further into carbon species which cannot be removed by deuterium. Indeed, the amount of carbonaceous species left on the surface after deuteration and removed by a subsequent oxygen treatment increases (5). Thus, the proportion of the highly dissociated species decreases. However, the amount of hydrogen leaving the dissociatively chemisorbed methane is high even at low temperature which is indicated by the high value of M_D . Provided that the temperature of chemisorption does not exceed 250°C, the major part of the CH_x can be removed by a hydrogen/deuterium treatment. Consequently, M_D represents the average hydrogen content of the CH_x species formed ($x=1$), which are the active species in the surface polymerization reaction to form higher hydrocarbons (6, 7).

Nevertheless, the method by which we determined the total amount of chemisorbed methane deserves further discussion. Belgued *et al.* determined the quantity of chemisorbed methane simply by hydrogenation (9). However, even after hydrogenation of the CH_x species, a part of it is retained by the surface of the metallic cobalt or ruthenium (5). This part may be completely nonreactive in the further surface transformation, but it is still a part of the carbon balance. This is why the method using oxygen, collecting the CO_2 and measuring it as the amount equal to the total chemisorbed methane, has been retained. This type of determination is difficult for the ruthenium-containing zeolite, because the oxygen treatment causes a change in the structure of the catalyst.

The further discussion will address two parameters: (i) the amount of methane chemisorbed and measured by oxidation to CO_2 and (ii) the number of hydrogen atoms lost after chemisorption and measured by deuterium uptake. Due to the strong carbon–metal interaction, some of the carbon is retained by the surface even after hydrogenation. This is a function of the metal and the metal/support interaction. We showed earlier that the higher the temperature for methane chemisorption, the greater amount of carbon retained after deuteration at 100°C (5).

The data on cobalt catalysts show that the support exerts a significant influence on the activation of methane. The amount of methane chemisorbed (Fig. 3) as well as the amount of hydrogen evolved (Fig. 4) decreases in the sequence $\text{Co}/\text{Al}_2\text{O}_3 > \text{Co}/\text{SiO}_2 > \text{Co}/\text{NaY}$. This sequence is related to the sequence of reducibility of the samples measured by temperature-programmed reduction (TPR) as was reported in the accompanying publication (19). It is well known that Co/NaY can hardly be reduced (15, 16) due to the migration of Co^{2+} ions into the hexagonal and sodalite

cages in which their reducibility is hampered by strong interactions with the surrounding framework ions. Although cobalt on silica is reducible (T_{\max} is about 400°C), it easily forms a stable cobalt silicate phase due to strong oxide–oxide interactions proposed by Lund and Dumesic for iron oxide/silica, i.e., incorporation of the Si^{4+} ions into the tetrahedral sites with formation of hydrotalcite-like silicate phases (21, 22).

Cobalt is reduced on alumina to the largest extent which can be attributed to the formation of a cobalt surface phase (CSP) which covers the alumina surface and promotes formation of a Co_3O_4 which is reducible (23–25). The metallic cobalt is often interfaced with oxide environments, and the amount of chemisorbed methane is less than over ruthenium-based catalysts. Nevertheless, dissociation of methane still takes place to a somewhat greater extent on cobalt than on ruthenium. This is also reflected in the hydrogen content of the deuterated species illustrated by the M_D values.

Consequently, the difference in methane activation results from the difficulty in reducing cobalt ions on the various supports. The large amount of hydrogen produced during the dissociative chemisorption of methane over $\text{Co}/\text{Al}_2\text{O}_3$ is also an indication of the large fraction of metallic cobalt particles on which hydrogen dissociation from CH_x proceeds into hydrogen-free carbon species.

Ruthenium appears to be less able to make highly dehydrogenated species than the cobalt samples, because the amount of CD_4 over Ru-containing catalysts is somewhat lower than that over cobalt. The sequence in activity to chemisorb methane is $\text{Ru}/\text{SiO}_2 > \text{Ru}/\text{NaY} > \text{Ru}/\text{Al}_2\text{O}_3$; this is again in accordance with the reducibility sequence (19). Previous studies indicated that ruthenium is active both in the hydrogenolysis of butanes (26) and in the CO hydrogenation, in particular when supported on silica. The catalysts discussed here were only oxygen treated which resulted in the formation of large ruthenium oxide crystallites and after hydrogenation, in large metal particles. While ruthenium particles easily split C–H bonds at higher temperature, the CH_x species formed over ruthenium contain more hydrogen atoms than those produced over cobalt. This is in agreement with Goodman's results who showed that on a ruthenium single crystal the most abundant species after methane chemisorption is CH (27).

Consequently, from the M_D value in $\text{CH}_x\text{D}_{(4-x)}$ a composition of CHD_3 is verified over silica- and alumina-supported cobalt and ruthenium samples which supports the high degree of dissociation with a slightly less M_D values for ruthenium than for cobalt. The reverse is true on NaY -supported samples which is likely a result of the extent of reduction. The difference between cobalt and ruthenium also exists in methane/deuterium exchange (28, 29), on metal films (20), and on silica-supported ruthenium (30). The M_D values for the different supports over a wide temperature

range also indicate that over ruthenium the formation of the multiply deuterated species becomes of increasingly important at higher temperatures.

In the accompanying paper (19) we illustrated by means of XPS work that the binding energy values for ruthenium in the Ru/NaY sample are slightly higher than for the bulk ruthenium metal (31) indicating the presence of small zero-valent ruthenium particles in the zeolite supercages, in agreement with other studies (<1 nm diameter (32), 2.5–3.5 nm diameter (33), 1.1 nm diameter (34)). This is the case when the $[\text{Ru}(\text{NH}_3)_6]^{3+}$ /NaY precursor is decomposed in helium before reduction. A similar treatment in oxygen results in migration of ruthenium containing species to the external surface where large oxide particles are formed (32–36).

Small ruthenium particles located in NaY zeolite supercages appear to be the most active for chemisorption of methane. Consequently, if (i) small metal (ruthenium) particles can be stabilized in the supercage of NaY and (ii) oxide/metal interfaces can be avoided, a zeolite is superior to other supports. Although metallic cobalt looks more active, its activity is dictated by its poor reducibility in NaY.

It is noteworthy that the nature of the metal also affects the C–H bond activation. Recently methane activation over Pt/SiO₂ and on Pt/NaY clearly showed that the formation of highly dissociated species are more favorable on ruthenium than on platinum (6). This is in accordance with deuterium exchange on platinum catalyst (37). In the case of ruthenium the increase in the M_D values with temperature may indicate further dissociation of the hydrogen atoms from the multiply bonded radicals. The percentage of isotopic products mainly CD₄ with CD₃H and CD₂H₂ suggests formation of α,α -diadsorbed species similarly to the multiple exchange (20).

The desorbing methane always has a certain distribution and there is no sharp maximum at a particular deuterium content. This is interpreted as follows. The metal sites on the surface also have a distribution controlled by surface morphology. The most active sites are occupied with the highly dissociated species and, sequentially, the less active sites are also covered by CH_x species. As the temperature increases further, dissociation occurs on the most active sites until they are blocked with hydrogen-free carbon species. Thus, the degree of dissociation of hydrogen from methane increases only slightly. This is why the average deuterium number, which is proportional to the degree of hydrogen dissociation, gives realistic information about the catalyst surface. The M_D values for cobalt and ruthenium are around 3, while, for example, platinum is significantly less, about 2 (6). Moreover, if the metal particles are reduced to a small extent, that is, if metal sites are surrounded by ionic species, the methane dissociation drastically decreases as occurred for Co/NaY.

We now turn our attention to the bimetallic catalysts. More recently we studied the effect of a second metal, platinum, which has greatly enhanced the activity of the Co/NaY catalyst in this low-temperature methane chemisorption and C₂₊ formation (6). Preliminary data on ruthenium–cobalt indicated a synergism in methane chemisorption compared to both Co/NaY and Ru/NaY (7). Since small ruthenium particles are created and stabilized in the Ru/NaY sample after helium treatment (23) the helium-treated samples are more active in C–H bond dissociation in methane than the oxygen-treated samples.

After helium treatment of the Ru–Co/NaY[II] sample (reduced in hydrogen and evacuated), the dissociative chemisorption of methane was observed at temperatures as low as 150°C, and the amount of methane chemisorbed is higher than on the sample treated in oxygen. This is the consequence of the morphology of metal particles discussed above. The high activity of the helium-treated sample could be explained by the extent of dehydrogenation of methane.

The gradual increase in the M_D value with temperature is due to the increase in the dissociative chemisorption of methane. The bimetallic system exhibits the highest activity, regardless of whether the sample is treated in helium or oxygen. It is interesting that M_D is always smaller for the He-treated sample than for the oxidized one, but the amount of CH_x is higher which means that small metal particles chemisorb methane in large amounts but in a less extensively dissociated form.

In the Ru–Co/NaY[II] system ruthenium is located in the external layer of the zeolite crystallites and thus, the migration of ruthenium to the external surface during oxygen treatment is very probable. This results in a small amount of methane chemisorption because of the lower number of sites for chemisorption. This problem was circumvented, at least to some extent, when Ru–Co/NaY[III] was applied. In this case the migration of ruthenium to the external surface might be controlled by the external cobalt layer during oxygen treatment. Even so, in helium-treated sample (Table 6) M_D is about 2, and this composition of the CH_x is more efficient for surface coupling. On the helium-treated sample the C₂₊ selectivity reached a maximum at very low conversions (3%), whereas on the oxygen-treated sample the C₂₊ selectivity increased to 35% but almost 70% methane was produced (7). This is likely due to the higher chain growing probability during methane chemisorption.

When the chemisorption of methane on helium-treated Ru/NaY, Co/NaY, and Ru–Co/NaY[III] samples is compared, the latter sample has the highest activity. This is in agreement with coupling results, i.e., C₂₊ selectivity reached a maximum of 92% with conversions up to 28%, while on the helium-treated Ru/NaY sample the C₂₊ selectivity was 85% with conversions up to only 8%. The difference between these two systems lies in the reducibility, the latter being reduced to a lesser extent than pure ruthenium. The

better coupling parameter of Ru/NaY is contrasted by the high instability of the small metal particles which is not the case for Ru-Co/NaY[III]. Although the amount of carbonaceous species built up on the ruthenium surface is higher than that on ruthenium-cobalt, it is less likely to be swept off by hydrogen than those on bimetallic particles (7).

In contrast, Ru/NaY shows higher methane chemisorption than Ru-Co/NaY[III] when calcined in oxygen. This is also in agreement with the coupling results. The yields on Ru/NaY (O₂ treated) reached 100% with almost 80% selectivity to C₂₊, whereas on the bimetallic system the C₂₊ selectivity was only 35% with 70% conversion (7). The differences in these samples are due to the difficulty in stabilizing the small metallic particles inside the zeolite matrix and to the differences in reducibility.

5. CONCLUSIONS

The capability of supported metal catalysts to C-H bond cleavage in methane can be estimated by using a method of deuterium uptake by the surface CH_x species formed after CH₄ chemisorption. The average deuterium number (M_D) is characteristic of the average degree of dissociation of methane.

The nature of the support affects the activation of methane by influencing the extent of metal reduction. Alumina-supported catalysts exhibit the highest activity on the basis of the amount of hydrogen evolved, while the highest amount of methane was chemisorbed on silica-supported ruthenium and alumina-supported cobalt samples.

The average deuterium number changes slightly with increasing temperature, although the amount of methane chemisorbed and the hydrogen evolved increases. This contradiction can be interpreted by the increasing amount of fully dissociated methane which occupies the most active sites of the metal surface.

The average deuterium number depends on the nature of the metal, while the total amount of chemisorbed methane is a function of both the metal and the support.

Ru-Co/NaY catalysts have the highest activity in dissociating methane provided that treatment of the precursor occurs in helium instead of oxygen. In the latter case ruthenium forms large metal particles on the external surface of the zeolite.

ACKNOWLEDGMENTS

The authors are indebted to the COST program (Grant D5/0001/93 and the National Science and Research Fund (Grant T-17046) and Professor I. Kiricsi provided the Ru-Co/NaY samples and participated in helpful discussion. K.V.S. is grateful to the Technical University in Budapest for supporting his Ph.D. work.

REFERENCES

1. Koerts, T., Deelen, M. J. A., and van Santen, R. A., *J. Catal.* **138**, 101 (1992).
2. Koerts, T., van Wolput, J. H. M. C., de Jong, A. M., Niemantsverdriet, J. W., and van Santen, R. A., *Appl. Catal.* **115**, 315 (1994).
3. Guczi, L., van Santen, R. A., and Sarma, K. V., *Catal. Rev. Eng. Sci.* **38**, 329 (1996).
4. Belgued, M., Pareja, P., Amariglio, A., and Amariglio, H., *Nature* **352**, 789 (1991).
5. Guczi, L., Sarma, K. V., Koppány, Zs., Sundararajan, R., and Zsoldos, Z., *Stud. Surf. Sci. Catal.*, in press.
6. Guczi, L., Sarma, K. V., and Borkó, L., *Catal. Lett.* **39**, 43 (1996).
7. Guczi, L., Koppány, Zs., Sarma, K. V., Borkó, L., and Kiricsi, I., "Progress in Zeolite and Microporous Materials" (H. Chon, S.-K. Ihm, and Y. S. Uh, Eds.), *Stud. Surf. Sci. Catal.* **105**, p. 861. Elsevier, Amsterdam, 1997.
8. Tanaka, K., Yaega, I., and Aomura, K., *J. Chem. Soc. Chem. Comm.*, 938 (1982).
9. Belgued, M., Amariglio, H., Pareja, P., Amariglio, A., and Saint-Just, J., *Catal. Today* **13**, 437 (1992).
10. Erdőhelyi, A., Cserényi, J., and Solymosi, F., *J. Catal.* **141**, 287 (1993).
11. Solymosi, F., Erdőhelyi, A., Cserényi, J., and Felvégi, A., *J. Catal.* **147**, 272 (1994).
12. Solymosi, F., and Cserényi, J., *Catal. Today* **21**, 561 (1994).
13. Cheikhi, N., Ziyad, M., Coudurier, G., and Vedrine, J. C., *Appl. Catal. A* **118**, 187 (1994).
14. Lu, G., Hoffer, T., and Guczi, L., *Catal. Lett.* **14**, 207 (1992).
15. Lu, G., Hoffer, T., and Guczi, L., *Appl. Catal.* **93**, 61 (1992).
16. Zsoldos, Z., Garin, F., Hilaire, L., and Guczi, L., *Catal. Lett.* **33**, 39 (1995).
17. Zsoldos, Z., Vass, G., Lu, G., and Guczi, L., *Appl. Surf. Sci.* **78**, 467 (1994); Lu, G., Zsoldos, Z., Koppány, Zs., and Guczi, L., *Catal. Lett.* **24**, 15 (1994).
18. Solymosi, F., and Cserényi, J., *Catal. Lett.* **34**, 343 (1995).
19. Guczi, L., Sundararajan, R., Koppány, Zs., Zsoldos, Z., Schay, Z., Niwa, S., and Mizukami, F., *J. Catal.* **167**, 482 (1997).
20. Kemball, C., *Adv. Catal.* **11**, 223 (1959).
21. Lund, C. R. F., and Dumesic, J. A., *J. Phys. Chem.* **85**, 3175 (1982).
22. Niemantsverdriet, J. W., van der Kraan, A. M., and Delgass, W. N., *J. Catal.* **89**, 138 (1984).
23. Zsoldos, Z., Hoffer, T., and Guczi, L., *J. Phys. Chem.* **95**, 798 (1991).
24. Guczi, L., Hoffer, T., Zsoldos, Z., Zyade, S., Maire, G., and Garin, F., *J. Phys. Chem.* **95**, 802 (1991).
25. Zsoldos, Z., and Guczi, L., *J. Phys. Chem.* **96**, 9393 (1992).
26. Bond, G. C., and Slaa, J. C., *J. Mol. Catal.* **98**, 81 (1995); Sinfelt, J. H., *Adv. Catal.* **23**, 91 (1973).
27. Lenz-Solomun, P., Woo, M.-C., and Goodman, D. W., *Catal. Lett.* **25**, 75 (1994).
28. McKee, D. W., and Norton, F. J., *J. Catal.* **3**, 252 (1964).
29. McKee, D. W., and Norton, F. J., *J. Phys. Chem.* **68**, 481 (1964).
30. Brown, R., and Kemball, C., *J. Chem. Soc. Faraday Trans. I* **89**, 585 (1993).
31. Shyu, J. Z., Goodwin, J. G., Jr., and Hercules, D. M., *J. Phys. Chem.* **89**, 4983 (1985).
32. Pedersen, L. A., and Lunsford, J. H., *J. Catal.* **61**, 39 (1980).
33. Wellenbücher, J., Rosowski, F., Kengler, U., Muhler, M., Ertl, G., Guntow, U., and Schlägl, R., in "Zeolites and Related Microporous Materials: State of the Arts 1994," *Stud. Surf. Sci. Catal.* (J. Weitkamp, H. G. Karge, H. Pfeifer, and W. Hölderich, Eds.), Vol. 84, p. 941. Elsevier, Amsterdam, 1994.
34. Ishihara, T., Harada, K., Eguchi, K., and Arai, H., *J. Catal.* **136**, 161 (1992).
35. Wellenbücher, J., Muhler, M., Mahdi, W., Sauerlandt, U., Schütze, J., Ertl, G., and Schlägl, R., *Catal. Lett.* **25**, 61 (1994).
36. Cho, I. H., Cho, S. J., Park, S. B., and Ryoo, R., *J. Catal.* **153**, 232 (1995).
37. Guczi, L., Sárkány, A., and Tétényi, P., *J. Catal.* **39**, 181 (1975).